In Silico Identification and Experimental Validation of Novel KPC-2 β-lactamase Inhibitors

R. Klein[a,f]§, P. Linciano[b]§, G. Celenza[c], P. Bellio[c], S. Papaioannou[b], J. Blazquez[d], L. Cendron[e], R. Brenk[f]* and D. Tondi[b]*.

[a] Institute of Pharmacy and Biochemistry, Johannes Gutenberg University, Staudinger Weg 5, 55128 Mainz, Germany.

[b] Dipartimento di Scienze della Vita, Università di Modena e Reggio Emilia, Via Campi 103, 41125, Modena, Italy.

[c] Dipartimento di Scienze Cliniche Applicate e Biotecnologie, Università dell'Aquila, Via Vetoio, 1, 67100 L'Aquila, Italy.

[d] Department of Microbial Biotechnology, National Center for Biotechnology, Consejo Superior de Investigaciones Científicas (CSIC), C/ Darwin, 3, Campus de la Universidad Autonoma-Cantoblanco, 28049-Madrid, Spain

[e] Dipartimento di Biologia, Università di Padova, Viale G. Colombo 3, 35121, Padova, Italy.

[f] Department of Biomedicine, University of Bergen, Jonas Lies vei 91, 5020 Bergen, Norway

§ Both authors contributed equally to this work.

* Corresponding authors. Email: tondi.donatella@unimore.it; Ruth.Brenk@uib.no

Abstract

Bacterial resistance has become a worldwide concern, particularly after the emergence of resistant strains overproducing carbapenemases. Among these, the KPC-2 carbapenemase represents a significant clinical challenge, being characterized by a broad substrate spectrum that includes aminothiazoleoxime and cephalosporins such as cefotaxime. Moreover, strains harboring KPC-type β-lactamases are often reported as resistant to available β-lactamase inhibitors (clavulanic acid, tazobactam and sulbactam). Therefore, the identification of novel non β-lactam KPC-2 inhibitors is strongly necessary to maintain treatment options. This study explored novel, non-covalent inhibitors active against KPC-2, as putative hit candidates. We performed a structure-based *in silico* screening of commercially available compounds for non-β-lactam KPC-2 inhibitors. Thirty-two commercially available high-scoring, fragment-like hits were selected for *in vitro* validation and their activity and mechanism of action *vs* the target was experimentally evaluated using recombinant KPC-2. N-(3-(1H-tetrazol-5-yl)phenyl)-3-fluorobenzamide (**11a**), in light of its ligand efficiency (LE = 0.28 kcal/mol/non-hydrogen atom) and chemistry, was selected as hit to be directed to chemical optimization to improve potency *vs* the enzyme and explore structural requirement for inhibition in KPC-2 binding site. Further, the compounds were evaluated against clinical strains overexpressing KPC-2 and the most promising compound reduced the MIC of the β-lactam antibiotic meropenem by four fold.

Introduction

The emergence of KPC-2 class-A Beta-Lactamase (BL) carbapenemase, which confers resistance to last resort carbapenems, poses a serious health threat to the public. KPC-2, a class A BL, uses a catalytic serine to hydrolyze the β-lactam ring. Specifically, the hydrolysis reaction proceeds through a series of steps involving: (i) the formation of a precovalent complex, (ii) the conversion to a high-energy tetrahedral acylation intermediate, (iii) followed by a low-energy acyl-enzyme complex, (iv) a high-energy tetrahedral de-acylation intermediate consequent to catalytic water attack, and (v) finally the release of the hydrolyzed β-lactam ring product from the enzyme. [1–6].

Notably to treat infections caused by bacteria that produce class A BLs, mechanism-based inhibitors (i.e., clavulanic acid, sulbactam, and tazobactam) are administered in combination with β-lactam antibiotics. However, strains harboring KPC-type β-lactamases are reported to be resistant to available β-lactamase inhibitors. Moreover, because of KPC-2's broad spectrum of activity (which includes penicillins, cephalosporins, and carbapenems) treatment options against KPC-2-producing bacteria are scarce, and "last-resort" carbapenems are ineffective as well [7]. Therefore, studies directed to the discovery of novel, non β-lactam KPC-2 inhibitors have multiplied in the last years. Recently, new drugs able to restore susceptibility to β-lactams i.e. the novel inhibitor avibactam in combination with ceftazidime (CAZ) and RPX7009 (vaborbactam) with meropenem have been approved (Fig. 1)[8-10].
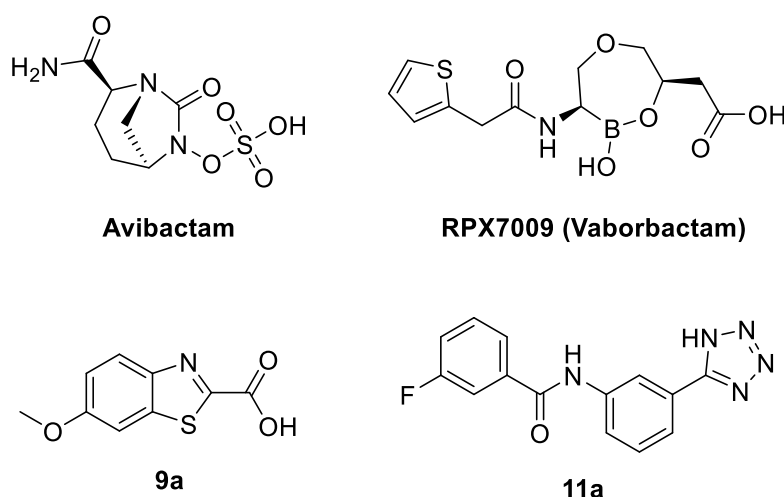
Figure 1. Chemical structure of avibactam, RPX7009, and compounds **9a** and **11a**

56   As attention on KPC-2 rises, the number of crystal structures of its apo and complexed form disclosed

57   in the PDB has increased, making KPC-2 a druggable target for structure based drug design efforts and

58   for the study of novel, non β-lactam like inhibitors of this threatening carbapenemase [9–12]

59   Recently, two crystal structures of the hydrolyzed β-lactam antibiotics cefotaxime and faropenem in

60   complex with KPC-2 were determined (PDB codes 5UJ3, 5UJ4; Fig. 2).[13]
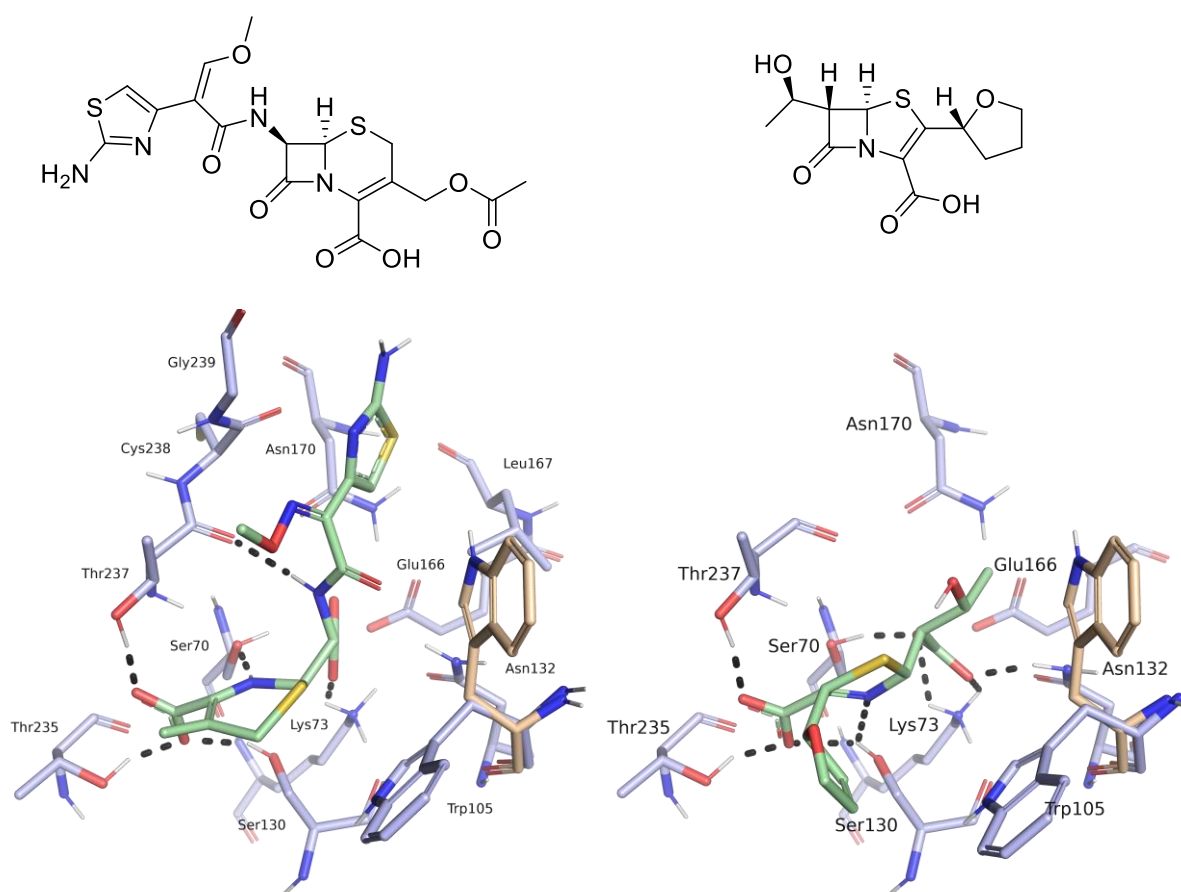
Figure 2. Structures and binding modes of hydrolyzed β-lactam antibiotics in the KPC-2 binding site. Left: binding mode of hydrolyzed cefotaxime (PDB code 5UJ3). Right: binding mode of hydrolyzed faropenem (PDB code 5UJ4). The second rotamer of Trp105 adopted in the apo-enzyme is coloured in beige, protein side chains in blue and ligands in green. Hydrogen bonds are indicated as black dots.

61

4

62 Both ligands form hydrogen-bond interactions with their C4-carboxyl group to Ser130, Thr235 and

63 Thr237. The dihydrothiazine moiety of cefotaxime and the dihydrothiazole moiety of faropenem forms

64 π-π-stacking interactions with Trp105. In the apo-enzyme, this side chain adopts two rotamers, upon

65 binding of a ligand just one. Mutagenesis studies have shown the importance of Trp105 in substrate

66 recognition [7]. The faropenem ring nitrogen forms a hydrogen-bond interaction with Ser130, whereas

67 the ring nitrogen of cefotaxime a hydrogen bond with Ser70. The aminothiazole ring of cefotaxime

68 forms van-der-Waals contacts with Leu167, Asn170, Cys238 and Gly239, while the oxyimino group

69 and the hydroxyethyl group of faropenem are solvent exposed (Fig. 2).[13]

70 Based on this and other structural information, we used a hierarchical screening cascade for the

71 discovery of non β-lactam like KPC-2 inhibitors. The selected candidates were then validated as hits

72 against isolated recombinant KPC-2. Among the tested compounds **9a**, a benzotiazole derivative, and

73 **11a**, a tetrazole-containing inhibitor, showed the highest activity against KPC-2 and behaved as

74 competitive inhibitors of the targeted carbapenemase (Fig. 1). Compound **11a** was subsequently directed

75 to chemical optimization to improve potency *vs* the enzyme and explore structural requirement for

76 inhibition in KPC-2 binding site. Further, the compounds were evaluated against clinical strains

77 overexpressing KPC-2 and the most promising compound reduced the MIC of the β-lactam antibiotic

78 meropenem by four fold.

79

Materials and Methods

Pharmacophore hypothesis

82 A search for similar binding sites of KPC-2 was carried out using the online tool PoSSuM - Search K

83 [15,16]. Based on shared ligand interactions in the retrieved structures (Table 1), a pharmacophore was

84 defined based on a *K. pneumoniae* KPC-2 protein structure (PDB code 3RXW) [17] and the ligand OJ6

85 of CTX-M-9 β-lactamase (PDB code 4DE1) [18]. The derived pharmacophore contained a hydrogen-

5

86   bond acceptor feature for interaction with Thr237, Thr235 and Ser130, a hydrophobic feature for π-

87   stacking with Trp105 and a hydrogen bond acceptor feature for interactions with Asn132 (Fig. 3).

88

89

90   **Table 1:** Result of PoSSuM Search K for similar binding sites. Structures with binding sites similar

91   with structure 3RXW in complex with a non-covalent ligand were reported.

	PDB-code	Protein name	Resolution	Ref.
1	4BD0	*E.coli* β-lactamase TOHO-1	1.21 Å	[19]
2	3G30	*E.coli* β-lactamase CTX-M-9a	1.8 Å	[20]
3	4DE1	*E.coli* β-lactamase CTX-M-9a	1.26 Å	[18]
4	4DDY	*E.coli* β-lactamase CTX-M-9a	1.36 Å	[18]
5	4DE3	*E.coli* β-lactamase CTX-M-9a	1.44 Å	[18]
6	4DDS	*E.coli* β-lactamase CTX-M-9a	1.36 Å	[18]
7	4DE0	*E.coli* β-lactamase CTX-M-9a	1.12 Å	[18]
8	4EUZ	*S.fonticola* β-lactamase SFC-1	1.08 Å	[21]
9	4DE2	*E.coli* β-lactamase CTX-M-9a	1.40 Å	[18]
10	3G35	*E.coli* β-lactamase CTX-M-9a	1.41 Å	[20]
11	3G32	*E.coli* β-lactamase CTX-M-9a	1.31 Å	[20]
12	3G2Y	*E.coli* β-lactamase CTX-M-9a	1.31 Å	[20]
13	3G31	*E.coli* β-lactamase CTX-M-9a	1.70 Å	[20]

92
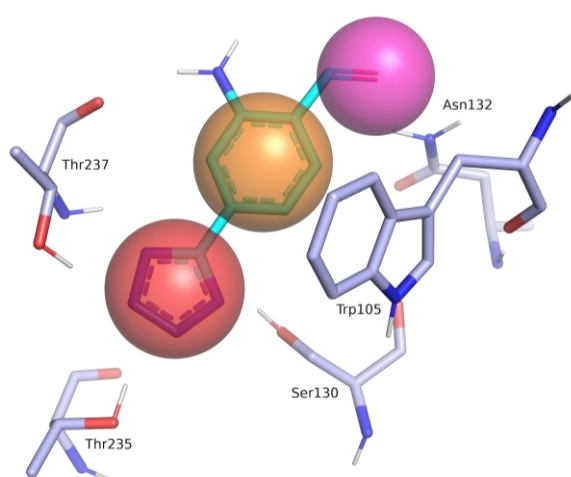
Figure 3. Binding site of KPC2 (PDB code 3RXW, blue) superimposed with a fragment of the ligand

OJ6 bound to CTX-M-9 β-lactamase (PDB code 4DE1, cyan) and pharmacophore features (red:

6

hydrogen-bond acceptor, orange: hydrophobic interaction feature, purple: hydrogen-bond donor) (Ambler numbering) [22].

Virtual Screening

94 Our in-house MySQL-database of commercially available compounds was filtered for compounds

95 fulfilling the following lead-like criteria: between 10 ten and 25 twenty-five heavy atoms, between one

96 and six hydrogen-bond acceptors, between one and three hydrogen-bond donors and a clog P between -

97 3 and 3. In addition, the complexity was limited by only including compounds with less than 7 rotatable

98 bonds and between 1 and 3 ring systems. Compounds containing unwanted reactive or toxic functional

99 groups were excluded as well [23].

100 In-house python scripts based on OpenEye's OEChem toolkit (OEChem, version 2016.6.1, OpenEye

101 Scientific Software, Inc., Santa Fe, NM, USA) were used to charge, tautomerize and stereoisomerize

102 the selected compounds. Conformers were generated using OpenEye's OMEGA toolkit [24]. The

103 pharmacophore filtering was carried out using Molecular Operating Environment (MOE, Chemical

104 Computing Group). Compounds that passed the pharmacophore filter were transformed into a format

105 suitable for docking as described previously [25].

106 The crystal structure of *K. pneumoniae* KPC-2 (PDB code 3RXW) [17] was used as receptor for

107 docking. The 'protonate 3D' tool of MOE was used to add polar hydrogen atoms to the receptor, energy

108 minimize their positions and to assign partial charges based on the AMBER force field parameters.

109 Water molecules and ligands (CIT and SR3) were deleted and the position of the Ser69 side chain was

110 energy minimized with the same force field parameters. The structure was aligned with the crystal

111 structure of *E.coli* CTX-M-9 (PDB code 4DE1) and the ligand 0J6 was used to define spheres as

112 matching points for docking. Grid-based excluded volume, van-der-Waals potential and electrostatic

113 potential as well as solvent occlusion maps were calculated as described earlier [26,27].

114 The compounds were docked into the binding site of KPC-2 using DOCK3.6 [27–29]. Parameters for

115 sampling ligand orientations were set as follows: bin size of ligand and receptor were set to 0.4 Å,

116 overlap bins were set to 0.2 Å and the distance tolerance for receptor and ligand matching spheres was

7

117   set to 1.5 Å. Each docking pose which did not overlap with the receptor was scored for electrostatic and

118   van-der-Waals complementarity and penalized according to its estimated partial desolvation energy. For

119   each compound, only the best-scoring pose out of its tautomers, protonation states or ring alignments

120   was saved in the final docking hit list. The docking hit list was filtered with the pharmacophore described

121   above, keeping the ligand positions rigid. Compounds passing this filter were ranked by their calculated

122   ligand efficiency [30,31] and inspected by eye.

123

Expression and purification of recombinant KPC-2.

125   The bla_{KPC-2} gene was kindly provided by Prof. Sergei Vakulenko (University of Notre Dame du Lac,

126   Indiana, USA) and cloned as already reported [32] and transformed into competent *E.coli* BL21 (DE3)

127   cells for protein expression. 50 mL of Tryptic Soy Broth (TSB) (50 mg/L kanamycin) were inoculated

128   with fresh colonies and grown at 37°C. 4 mL of the overnight culture was used to inoculate 1.3 L of

129   TSB (50 mg/L kanamycin) grown at 37°C with shaking to an optical density of 0.5 measured at 600 nm.

130   Then expression of recombinant *bla* gene was induced by adding 1.0 mM IPTG (isopropyl-D-

131   thiogalactopyranoside) and the cells were again allowed to grow at 20 °C overnight. Bacteria were

132   harvested by centrifugation at 4000 rpm for 20 minutes. The pelleted cells were resuspended in Tris-

133   HCl 50 mM pH 7.4-7.5. Periplasmatic proteins were extracted as reported in the pET System Manual

134   (TB055 10th Edition Rev. B 0403) and subsequently dialyzed in sodium acetate buffer (50 mM, pH

135   5.0). The protein was conveniently purified in a single step using a Macro-Prep High S resin and eluted

136   using sodium acetate 50 mM pH 5.0 and a sodium chloride (NaCl) linear gradient from 100 to 500 mM.

137   The purified protein was dialyzed overnight in sodium phosphate buffer 50 mM, pH 7.0 [32,33].

138

Inhibition Assays

140   The hydrolytic activity of KPC-2 activity was measured using the β-lactam substrates CENTA (100 uM,

141   K_M 70 uM) or nitrocefin (114 uM, K_M 36 µM) in reaction buffer consisting of 50 mM of PB at pH 7.0

142   at 25°C with 0.01% v/v Triton X-100 to avoid compound aggregation and promiscuous inhibition.[34]

8

143   Reactions were monitored using a Beckmann DU640® spectrophotometer at 405nM for CENTA and

144   480 nM wavelength for nitrocefin [35]. The test compounds were synthesized as described below or

145   purchased from Enamine, TimTec, Vitas-M, ChemBridge, Otava, Life Chemicals or Apollo Scientific

146   and assayed without further purification. Compounds were dissolved in dimethyl sulfoxide (DMSO) to

147   a concentration of 25 mM and stored at -20°C. The highest concentration at which the compounds were

148   tested was up to 1 mM (depending on their solubility). All experiments were performed in duplicate and

149   the error never exceeded 5%. The reaction was typically initiated by adding KPC-2 to the reaction buffer

150   last. To control for incubation effects, protein was added to the reaction buffer first, and the reaction

151   was initiated by the addition of reporter substrate after 10 minutes of enzyme-compound incubation.

152   The results are reported in Tables 2 and Table 3.

153   Competitive inhibition mechanism and the K_i for compound **9a** was determined by Lineweaver–Burk

154   (LB) and Dixon plots. For compound **11a**, already reported as competitive inhibitor of the extended

155   spectrum β-lactamase (ESBL) CTX-M15, the K_i was calculated by the Cheng-Prusoff equation (K_i=

156    $IC_{50}/(1+ [S]/K_M)$ assuming competitive inhibition [36].

157

Synthetic procedures

158

159   All commercially available chemicals and solvents were reagent grade and were used without further

160   purification unless otherwise specified. Reactions were monitored by thin-layer chromatography on

161   silica gel plates (60F-254, E. Merck) and visualized with UV light, cerium ammonium sulfate or alkaline

162    $KMnO_4$ aqueous solution. The following solvents and reagents have been abbreviated: ethyl ether

163   (Et_2O), dimethyl sulfoxide (DMSO), ethyl acetate (EtOAc), dichloromethane (DCM), methanol

164   (MeOH). All reactions were carried out with standard techniques. NMR spectra were recorded on a

165   Bruker 400 spectrometer with ^{1}H at 400.134 MHz and ^{13}C at 100.62 MHz. Proton chemical shifts were

166   referenced to the TMS internal standard. Chemical shifts are reported in parts per million (ppm, δ units).

167   Coupling constants are reported in units of Hertz (Hz). Splitting patterns are designed as s, singlet; d,

168   doublet; t, triplet; q quartet; dd, double doublet; m, multiplet; b, broad. Mass spectra were obtained on

169   a 6520 Accurate-Mass Q-TOF LC/MS and 6310A Ion TrapLC-MS(n).

170

General procedure for the synthesis of sulfonamides 1-6b

To a solution of 3-(1H-tetrazol-5-yl)aniline (1 eq.) in DCM dry (25 mL) at room temperature and under nitrogen atmosphere, pyridine (3 eq.) and the appropriate sulfonyl-chloride (1.2 eq.) were added. The mixture was reacted at room temperature for 2-12 h. The reaction was quenched with aqueous satured solution of NH_4Cl and acidified at pH 4 with aqueous 1N HCl. The aqueous phase was extracted with AcOEt, and the organic phase washed with brine, dried over Na_2SO_4 and concentrated. The crude was crystalized from MeOH or Et_2O to give the desired product.

N-(3-(1H-tetrazol-5-yl)phenyl)-3-fluorobenzenesulfonamide (1b)

Pale yellow solid (150 mg, yield 47%). ^{1}H NMR (400 MHz, DMSO-d6) δ 7.19 (dd, J = 2.2, 8.1 Hz, 1H), 7.33 – 7.45 (m, 2H), 7.47 – 7.58 (m, 3H), 7.62 (d, J = 7.7 Hz, 1H), 7.76 (t, J = 1.8 Hz, 1H), 10.61 (s, 1H), the H of tetrazole exchanges. MS m/z [M+H]$^+$ 320.1; [M-1]$^-$ 318.0.

N-(3-(1H-tetrazol-5-yl)phenyl)-3-nitrobenzenesulfonamide (2b)

Pink solid (62% yield). ^{1}H-NMR (400 MHz, DMSO-d6) δ: 7.31 (ddd, J = 1.0, 2.3, 8.2 Hz, 1H), 7.51 (t, J = 8.0 Hz, 1H), 7.74 (dt, J = 1.2, 7.8 Hz, 1H), 7.82 – 7.96 (m, 2H), 8.18 (dt, J = 1.3, 7.9 Hz, 1H), 8.46 (ddd, J = 1.0, 2.3, 8.2 Hz, 1H), 8.54 (t, J = 2.0 Hz, 1H), 10.90 (s, 1H); the H of tetrazole exchanges. ^{13}C-NMR (DMSO-d6) δ: 117.35, 120.09, 123.04, 127.35, 129.17, 129.22, 129.69, 133.21, 136.59, 137.99, 139.81, 148.82, 154.28. MS m/z [M+H]$^+$ Calcd for $C_{13}H_{10}N_6O_4S$: 346.0 Found: 347.2.

N-(3-(1H-tetrazol-5-yl)phenyl)-5-(dimethylamino)naphthalene-1-sulfonamide (3b)

White solid (31% yield). ^{1}H NMR (400 MHz, DMSO-d6) δ 2.78 (s, 6H), 7.20 (dd, J = 1.5, 7.6 Hz, 1H), 7.24 – 7.38 (m, 3H), 7.39 – 7.65 (m, 3H), 8.27 (dd, J = 1.6, 7.5 Hz, 1H), 8.41 (ddd, J = 1.5, 7.5, 19.3 Hz, 2H), the H of tetrazole exchanges. MS m/z [M+H]$^+$ Calcd for $C_{19}H_{18}N_6O_2S$: 394.1 Found: 395.1.

N-(4-(N-(3-(1H-tetrazol-5-yl)phenyl)sulfamoyl)phenyl)acetamide (4b)

Pink solid (52% yield). ^{1}H NMR (400 MHz, DMSO-d6) δ 2.12 (s, 3H), 7.31 (ddd, J = 1.0, 2.3, 8.2 Hz, 1H), 7.44 (t, J = 7.9 Hz, 1H), 7.65 – 7.72 (m, 3H), 7.74 – 7.79 (m, 2H), 7.86 (t, J = 1.9 Hz, 1H), the H of tetrazole exchanges. ^{13}C NMR (100 MHz, DMSO-d6) δ 22.58, 118.86, 118.95, 122.60, 123.07,

197   126.32, 127.96, 128.87, 129.96, 133.69, 139.01, 142.97, 170.57. MS m/z [M+H]$^+$ Calcd for

198    $C_{15}H_{14}N_6O_3S$: 358.1 Found: 359.2.

N-(3-(1H-tetrazol-5-yl)phenyl)quinoline-8-sulfonamide (5b)

200   White solid (88% yield). ^{1}H NMR (400 MHz, Acetone-d6) δ 7.28 – 7.42 (m, 2H), 7.59 – 7.90 (m, 4H),

201   8.03 (dt, J = 1.1, 1.8 Hz, 1H), 8.25 (dd, J = 1.5, 8.2 Hz, 1H), 8.42 (dd, J = 1.4, 7.3 Hz, 1H), 8.52 (dd, J

202   = 1.8, 8.4 Hz, 1H), 9.21 (dd, J = 1.8, 4.3 Hz, 1H), 9.41 (s, 1H), the H of tetrazole exchanges. ^{13}C NMR

203   (100 MHz, Acetone-d6) δ 117.35, 120.09, 123.01, 123.04, 125.55, 128.06, 129.17, 129.69, 129.79,

204   130.11, 133.27, 139.81, 140.02, 140.84, 149.72, 154.28. MS m/z [M+H]$^+$ Calcd for $C_{16}H_{12}N_6O_2S$: 352.1

205   Found: 353.2.

N-(3-(1H-tetrazol-5-yl)phenyl)-4-chlorobenzenesulfonamide (6b)

207   Light yellow solid (93% yield). ^{1}H NMR (400 MHz, Methanol-d4) δ 7.57 (t, J = 8.0 Hz, 1H), 7.74 (dt,

208   J = 1.3, 7.9 Hz, 2H), 7.78 – 7.84 (m, 1H), 7.99 (d, J = 8.6 Hz, 2H), 8.06 (d, J = 8.6 Hz, 2H), 8.41 (t, J =

209   1.9 Hz, 1H), the H of tetrazole exchanges. ^{13}C NMR (100 MHz, Methanol-d4) δ 117.35, 120.09, 123.01,

210   123.04, 125.55, 128.06, 129.17, 129.69, 129.79, 130.11, 133.27, 139.81, 140.02, 140.84, 149.72,

211   154.28. MS m/z [M+H]$^+$ Calcd for $C_{13}H_{10}ClN_5O_2S$: 335.0, 337.0 Found: 336.1, 338.2.

212

Results and Discussion

Virtual Screening

215   The binding sites in the available KPC-2 crystal structures were analyzed to select a suitable receptor

216   for docking. Alignment and superposition of the binding site residues of the seven available crystal

217   structures of *E.coli* and *K. pneumoniae Kp*KPC-2 revealed a rather rigid binding site with only Trp105

218   adopting two different rotamers, a closed conformation found 6-times and an open one, found two-

219   times. In one structure, both rotamers were present (Fig.4). Thus, for virtual screening, the structure with

220   the highest resolution was selected (*K. pneumoniae* KPC-2 in complex with the covalent inhibitor

221   penamsulfone PSR-3-226 (PDB code 3RXW), 1.26 Å resolution). This structure contained both

222   rotamers of Trp105. For virtual screening, the closed conformation was chosen, as this is the most

223   dominant conformation upon ligand binding.

11
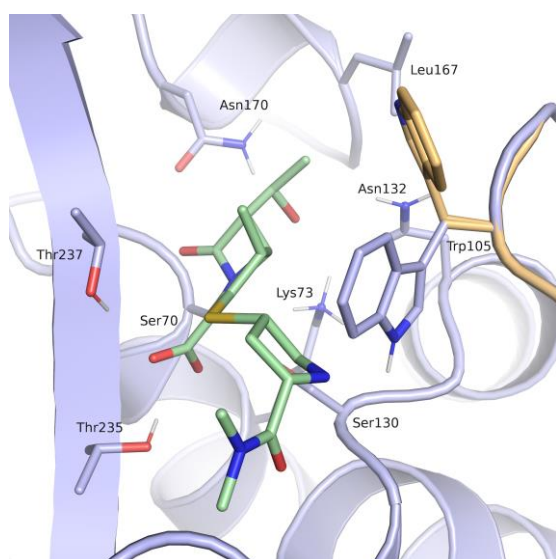
Figure 4. Binding site of *Kp*KPC2 (PDB code 3RXW) with ligand meropenem (green, PDB code 4EUZ). The receptor conformation used for docking is coloured in blue, the rotamer of Trp105 not considered in the docking setup in beige (Ambler numbering) [22].

224

225 Only little diversity with respect to bound ligands was found in the *Kp*KPC2 structures. To obtain a

226 more detailed picture on key interactions and to derive a pharmacophore hypothesis, PoSSuM - Search

227 K was used to search for similar binding sites containing non-covalent ligands. This resulted in thirteen

228 structures (Table 1), all having tetrazoles or carboxylates derivatives bound in the hydrophilic pocket

229 formed by the amino acids corresponding to Thr235, Thr237, Ser130 and Ser70 in *Kp*KPC2 (Fig.4).

230 Seven of the contained ligands were fragment hits for *E.coli* CTX-M class A extended spectrum β-

231 lactamase (ESBL), and four were derivatives of the most potent screening hit. Further, a structure of *S.*

232 *fonticola* SFC-1 S70A β-lactamase in a non-covalent complex with meropenem and one of *E.coli* Toho-

233 1 R274N: R276N β-lactamase in complex with a boronic acid were retrieved. Superposition of the

234 binding site residues of *Kp*KPC-2 (PDB code 3RXW) and the CTX-M β-lactamase structures gave rmsd

235 values for the Cα atoms between 0.72 and 0.82 Å, for superposition of *Kp*KPC-2 and *S. fonticola* SFC-

236 1 (PDB code 4EUZ) 0.28 Å and for superposition *Kp*KPC-2 and *E.coli* Toho-1 (PDB code 4BD0) 0.73
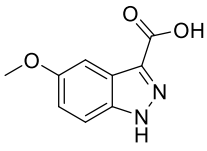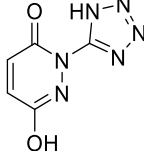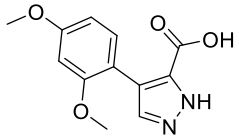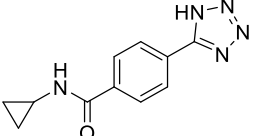
237 Å (Fig. 5).

12
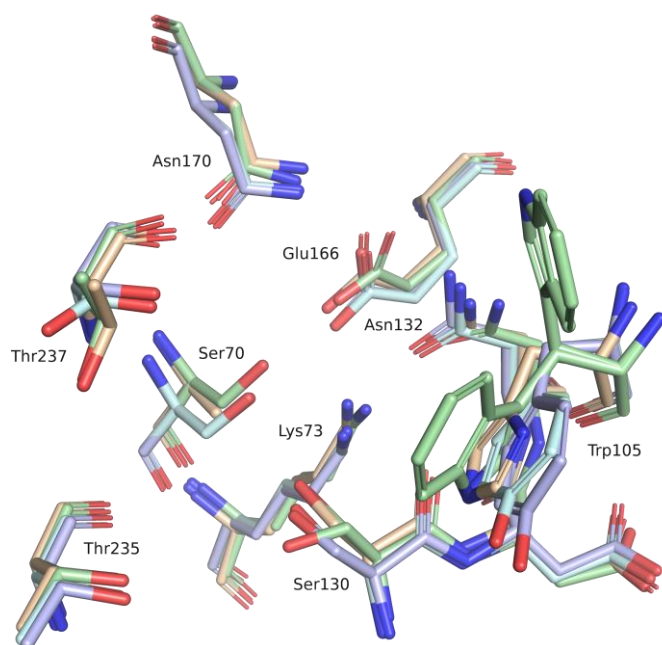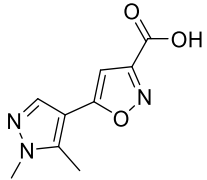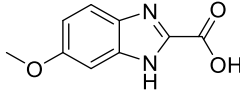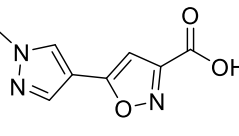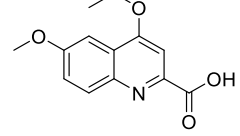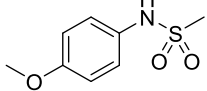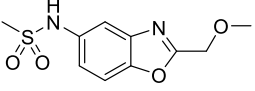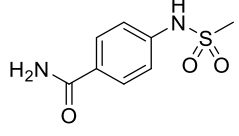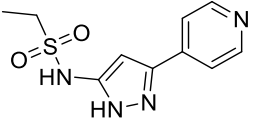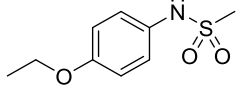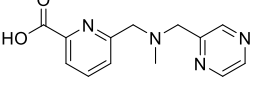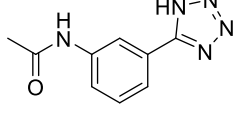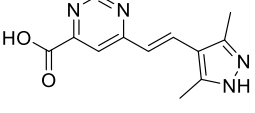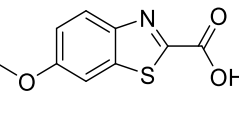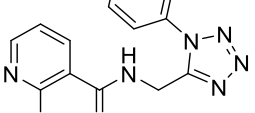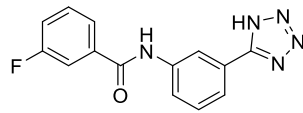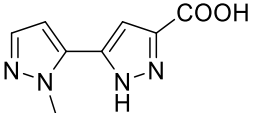
Figure 5. Superposition of the *Kp*KPC-2 binding site residues (PDB code 3RXW, green) with the *E.coli* CTX-M-9 β-lactamase (PDB code 4DDS, blue), the *S.fonticola* SFC-1 β-lactamase (PDB code 4EUZ, beige) and the *E.coli* TOHO-1 β-lactamase (PDB code 4BD0, cyan) (Ambler numbering) [22].

238

239   Based on the retrieved structures, a pharmacophore hypothesis was derived. All of the ligands in these

240   structures as well as the β-lactamase binding protein (PDB code 3E2L, 3E2K) and the covalent ligand

241   of the structure used as receptor, formed a hydrogen-bond with Thr235 or Thr237. Accordingly, a

242   hydrogen-bond acceptor at the corresponding ligand position was considered to be crucial for binding

243   (Fig. 3). Further, in most of the structures the ligands formed interactions with Trp105 (*Ambler*

244   numbering) [22]. Therefore, this interaction was also included in the pharmacophore hypothesis.

245   Hydrogen-bond interactions to Asn130 were found in four structures (PDB codes 3RXW, 3G32, 3G30,

246   4EUZ) and included as well.

247

248   A hierarchical approach was adopted for virtual screening. First, our in-house database of around five
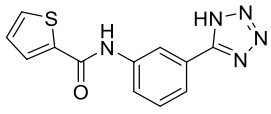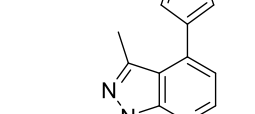
249   million purchasable compounds was filtered for lead-like molecules [23]. In the second step, the

250   obtained hits were screened with the above-described pharmacophore resulting in 44658 compounds.

251   Out of these, 31122 compounds could be docked into the *Kp* KPC2 binding site. Filtering these binding

13

252 poses again with the pharmacophore resulted in 2894 compounds. These were divided into three

253 clusters, depending on the functional group placed in the hydrophilic pocket (tetrazoles, carboxylates,

254 sulfonamides) and inspected by eye. Finally, 31 compounds were selected for hit validation (Table 2).

255 Most of the selected chemotypes carried an anionic group, mainly a carboxylic group or its bioisostere,

256 the tetrazole ring. Candidates were predicted to orient the anionic side of their moiety in the carboxylic

257 acid binding site of KPC-2, delimited by Ser130, Thr235 and Thr237 and present in all serine-based

258 Beta-lactamases. In the above mentioned site, in fact, binds the C(3)4' carboxylate of β-lactams

259 antibiotics as well as the sulfate group of avibactam and the carboxylic group of other known BLs

260 inhibitors [12,32,37,38,39].

261

Table 2. Inhibitory activity of compounds selected from virtual screening.

ID	Structure	IC_{50} mM [a,b]	ID	Structure	IC_{50} mM [a,b]
1a		> 0.33 (30)	17a		>1.0 (23)
2a		> 0.50 (38)	18a		1.0 (18)
3a		>0.25 (13)	19a		0.88
4a		>0.25 (12)	20a[c]		>0.5 (28)
5a		>0.50 (13)	21a		>1.0 (12)
6a		>1.0 (18)	22a		NI at 1.0
7a		>1.0 (12)	23a		>1.0 (26) [c]
8a		>0.50 (37)	24a		>0.1 (41)
9a[b]		0.15[c]	25a		> 0.4 (26)
10a[b]		0.07 [c]	26a		> 0.83 (18)
11a[b]		0.036 [c]	27a		NI at 0.5

15

| Compound	Value	Compound	Value
12a[b]	0.70 [c]	28a	>0.5 (14)
13a	NI at 0.25	29a	>1.0 (15)
14a	>1.0 (26)	30a	NI at 1.0
15a	>0.66 (38)	31a	>1. 0 (11)
16a	>1.0 (17)	32a	1.24

[a]Assays were performed in duplicate (errors were less than 5%) with CENTA as reporter substrate (100 μM, km 70 μM). Kinetic were monitored at 25° by following the absorbance variation at $\lambda = 405$ nm. [b] If no IC_{50} has been measured, percent inhibition at the highest tested concentration is given in parentheses. For example, > 0.50 (26 %) implies that the highest concentration tested was 0.50 mM; at this concentration, the enzyme was inhibited by 26 %. Therefore, IC_{50} > 0.50 mM. When % Inhibition was below 10% No Inibition (NI) is reported in table. [c]Assays were run after 10' incubation of the inhibitor with KPC-2. Reaction was started by the addition of CENTA.

262

Hit Evaluation

263

264 The majority of the selected candidates were fragment-like as defined by the "rule of three" [14]. Thus,

265 potencies in the high micromolar to millimolar range were expected. Unfortunately, the required high

266 concentrations for ligand testing could not always be achieved due to solubility issues which might have

267 resulted false negatives after testing. However, some of the tested molecules inhibited the hydrolytic

268 activity of KPC-2 with millimolar potency. Among those, compounds **9a** and **11a** were the most

269 promising compounds with micromolar affinities (IC_{50} of 0.15 and 0.036 mM, translating to ligand

270 efficiencies (LE) of 0.38 and 0.28 kcal/mol/non-hydrogen atom, respectively; Table 2) and were thus

271 further investigated.

272 Compound **9a** was predicted to place its carboxylate group in proximity of the catalytic Ser70, in the

273 carboxylic acid binding site mentioned above, forming hydrogen bond interactions with the side chains

274 corresponding to amino acids Ser130, Thr235 and Thr237 (Fig. 6). Thr 237 in KPC-2 is known to be

275 necessary for cephalosporinase and carbapenemase activity and is involved in clavulanic acid, sulbactam

276 and tazobactam recognition.[7] This position in β-lactamases that do not have carbapenemase or

277 extended-spectrum b-lactamase (ESBL) activity generally corresponds to an alanine. The side chain

278 hydroxyl groups of Ser130 and Ser70 were predicted to form interactions with the nitrogen of the

279 benzothiazole ring. The predicted position of the aromatic system is well placed to establish ring-ring

280 interactions with Trp105, a residue involved, in turn, in the stabilization of β-lactams through mainly

281 hydrophobic and van der Waals interactions (centroids distances of 4.4 and 4.5 A between Trp105 and

282 the thiophene and the benzene rings respectively) The role of Trp105 in substrate and inhibitor

283 interactions in KPC-2 β-lactamase has been deeply investigated being essential for hydrolysis of

284 substrates.[7] The methoxy group of the molecule is oriented towards a rather open and solvent

285 accessible area of the binging site and does not contact any of the surrounding residues. Interestingly,

286 the presence of the sulphur atom of the benzothiazole system seems critical for affinity as the related

287 compound **19a**, the benzimidazole analog, resulted 6-fold less active. Similar, the presence of the

288 carboxylic group appeared to be crucial as compound **32a,** without such a functionality, was 8-fold less

289 active.
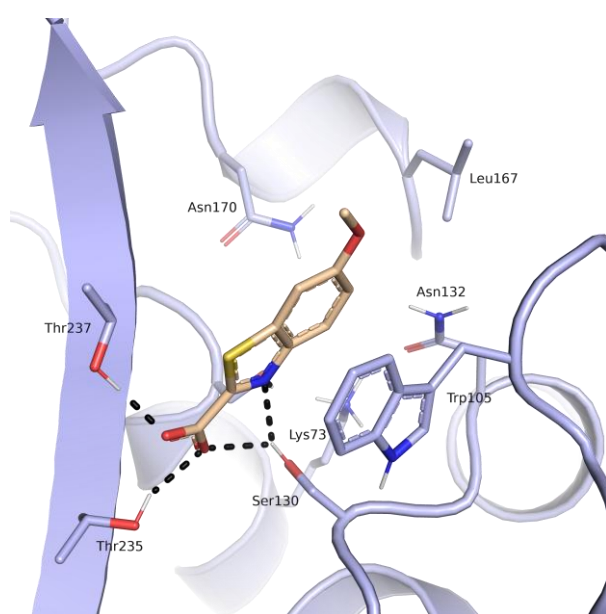
Figure 6. Predicted binding mode of compound **9a** (beige) in the *Kp*KPC-2 receptor (blue). Putative hydrogen bond interactions are indicated as black dots (Ambler numbering)[22].

290

291 For compound **9a** binding affinity and mode of inhibition was determined by using gradient

17

292 concentrations of CENTA. Fitting of the obtained data showed that compound **9a** behaves as a

293 competitive inhibitor with a determined *Ki* of 112.0 μM (Fig. 7). Its binding affinity was also determined

294 towards other class A β-lactamases (*IC$_{50}$* vs CTX-M9 160 μM). For this compound aggregating behavior

295 was also excluded by dynamic light scattering experiment (data not shown) [40]. Compound **9a** with its

296 fragment-like characteristic (MW 208.21, determined *Ki* 112.0 μM, LE 0.38 kcal/mol/non-hydrogen

297 atom) exerts an interesting activity *vs* KPC2-2 and represents a very promising molecule to be directed

298 to hit to lead optimization.
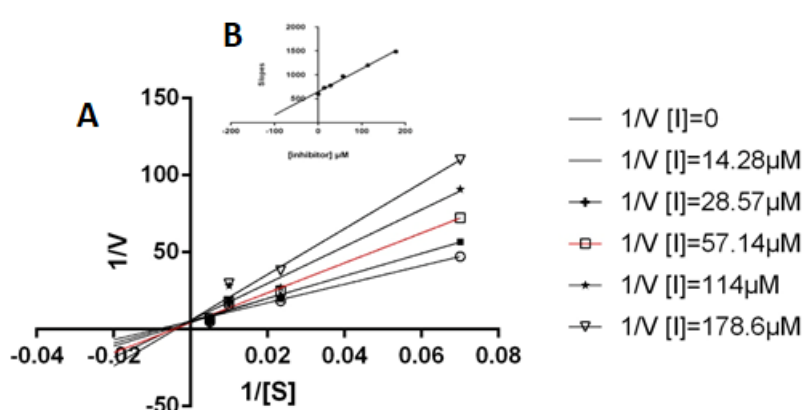
Figure 7. (A) Lineweaver–Burk plot **(A)** and Dixon slope plot **(B)** for competitive inhibitor, compound **9a**.

299

300 Among the 32 selected hits evaluated *in vitro* for their binding affinity vs KPC-2, compound **11a** was

301 the most active inhibitor with a micromolar affinity vs KPC-2 (determined *IC$_{50}$* 36 μM, calculated K*i*

302 14.8 μM, LE 0.28 kcal/mol/non-hydrogen atom).[36] The tetrazole ring of compound **11a**, a well-known

303 bioisostere of the carboxylic group, was predicted to lie in the hydrophilic pocket formed by Thr235,

304 Thr237, Ser130 and Ser70, driving the binding of the inhibitor in KPC-2 active site(Fig. 8). The phenyl

305 ring attached to the tetrazole was predicted to be sandwiched between the Trp105 side with a distance

306 compatible with weak hydrophobic interactions and the backbone of Thr237**.** The amide group of **11a**

307 was oriented in the canonical site delimited by Asn132, Asn170 and in a further distance Glu166 where

308 the R1 amide side chain of β-lactams is known to bind. However, the amine linker and the second phenyl

309 ring in **11a** were not predicted to form any specific interactions with the protein, except for the amide

310   nitrogen contacting the backbone of Thr237. The distal fluoro-benzene ring was oriented at the entrance

311   of the active site against two hydrophobic patches, one defined by Leu167, closer, and the other by the

312   backbone of Asn170, a residue critical for carbapenemase activity.
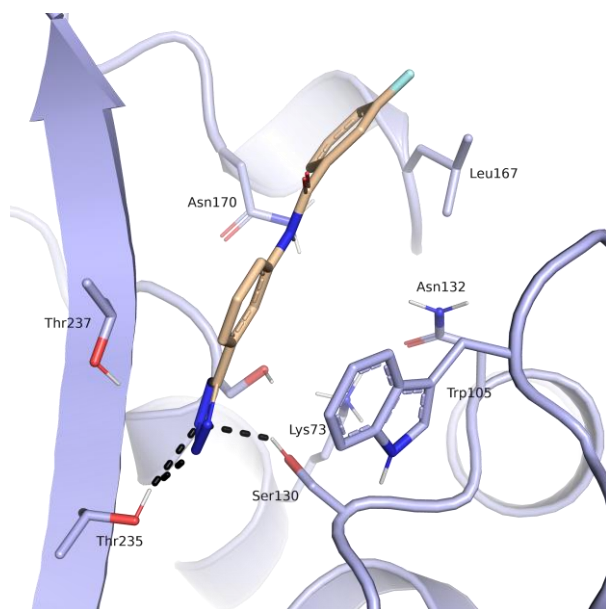
Figure 8. Predicted binding mode of compound **11a** (beige) in the *Kp*KPC-2 receptor (blue). Putative hydrogen bond interactions are indicated as black dots (Ambler numbering)[22].

313

314   Based on the predicted binding mode, the tetrazole group of **11a** seemed to be crucial for affinity. (Table

315   1). Moreover, while the proximal ring appeared to be involved in specific interactions, the amide group

316   and the distal ring did not contact efficaciously the protein. Based on predicted binding mode, chemical

317   size, synthetic accessibility for a rapid structural optimization and ligand efficacy compound **11a** was

318   directed to chemical synthesis development to improve its affinity and to investigate target binding

319   requirements for optimal inhibitor-enzyme interaction.

Hit derivatization and evaluation

321   In order to improve the binding affinity of **11a,** the compound was subjected to a hit optimization

322   program. Therefore, the phenyl-tetrazole moiety, that seemed to strongly drive the binding, was retained

323   unaltered, whereas structural modifications on the linker and on the distal aromatic ring were introduced

324   in order to explore and maximize the interactions with the pocket formed by Asn132, Asn170 and

325   Leu167 (Fig. 6). Because the amide linker does not contact efficaciously the protein we chose to replace

326   it with a sulfonamide (Fig. 9). We meant to target residues proximal to the opening of the active site

327   while investigating the potentiality for sulfonamide derivatives.

328
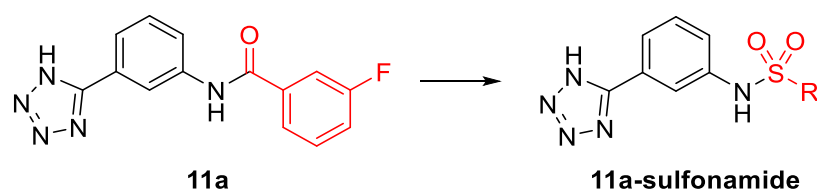
Figure 9. Virtual Screening hit **11a** (left), amine 1 (black) and the optimized part of the molecule (red).

329
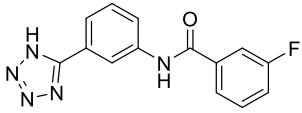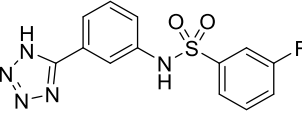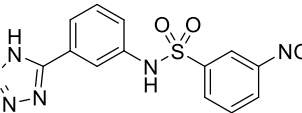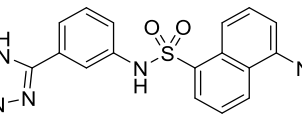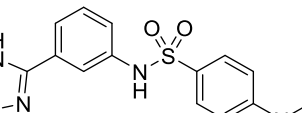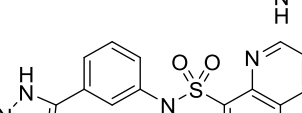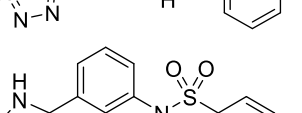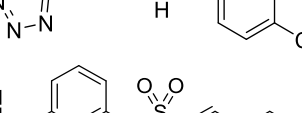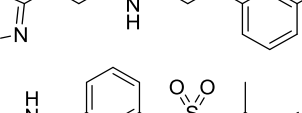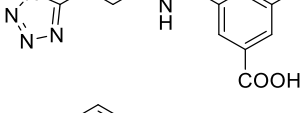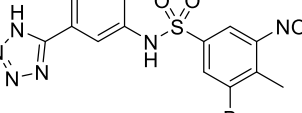
330   Sulfonamides are more stable towards hydrolysis than carboxyamides, possess an additional hydrogen

331   bonding oxygen atom and their NH is a strong hydrogen bond donor. In addition, the dihedral angle 'ω'

332   OSNH measures around 90° compared with the 180° 'ω' OCNH angle of amide. Sulfonamides, in

333   addition, have a non-planar configuration that could orient the distal ring towards Leu167 and Asn170

334   (Fig. 10). Therefore, the introduction of a sp^3 geometry could allow a more efficacious spanning of the

335   active site compared to the planar amide [41]. Moreover, modeling suggested that the sulfonamide group

336   could form an additional hydrogen bond with Asn132 residue actively involved in substrate recognition

337   and hydrolysis.

338

339

20

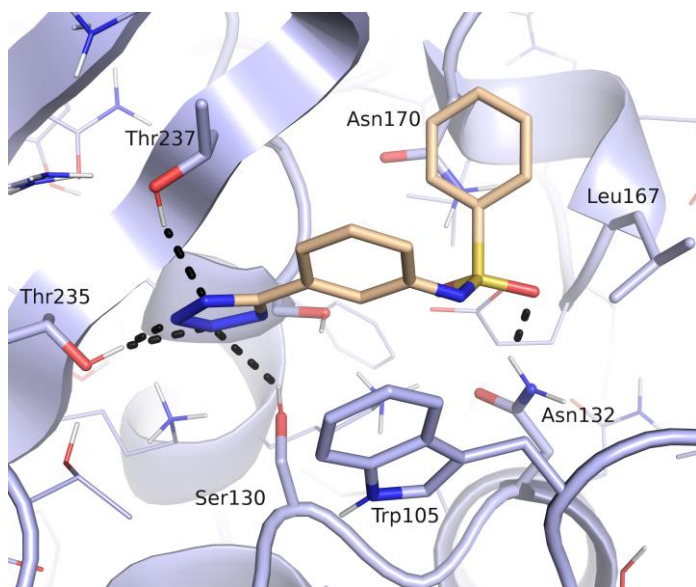**Figure 10.** Predicted binding mode of a sulfonamide derivative of compound **11a** (beige) in the *Kp*KPC-2 receptor (blue). Putative hydrogen bond interactions are indicated as black dots (Ambler numbering)[22].

340   Further, we explored different substitutions on the sulfonamide linker to probe binding interactions.

341   Substituents with different electronic and steric properties (i.e. halogens, nitro, sulfonamide, carboxylic

342   acid, methyl, acetamide, amino groups) were inserted in the different position of the aromatic ring. In

343   addition, the benzene ring was replaced by heterocyclic or extended benzofused systems such as

344   benzimidazole, quinazolinone, naphthalene, or quinolone ring. Based on the availability of compound

345   or building blocks, 6 compounds (**1b-6b**) were synthesized and 8 compounds (**7b-14b**) were purchased

346   to test our hypothesis (Table 3). The fourteen new compounds were tested *in vivo vs* clinical strains

347   overproducing KPC-2 to evaluate their ability to restore bacteria susceptibility to carbapenem

348   meropenem (Table 4).

349

21

Table 3: Inhibitory activity of **11a** sulphonamide derivatives.

ID	STRUCTURE	IC_{50} mM [a,b]
11a		0.036
1b		> 0.2 (25)
2b		>0.6 (23)
3b		Not tested not soluble
4b		> 0.2 (16)
5b		> 0.2 (13)
6b		NI at 0.2
7b		>1.0 (30)
8b		> 1.0 (37)
9b		NI at 0.5
10b		NI at 0.5

22

11b		> 1.0 (37)
12b		NI at 0.5
13b		NI at 0.5
14b		>500 (20)

[a]Assays were performed in duplicate (errors were less than 5%) with nitrocefin (114.28 μM, K_m 36 μM) as reporter substrate Kinetic were monitored at 25° by following the absorbance variation at $\lambda = 485$ nm. [b] If no IC_{50} has been measured, percent inhibition at the highest tested concentration is given in parentheses. For example, > 1.0 (37 %) implies that the highest concentration tested was 1.0 mM; at this concentration, the enzyme was inhibited by 37 % and IC_{50}> 1.0 mM. When % Inhibition was below 10% No Inhibition (NI) is reported in table.

Compounds **1b-6b** were synthesized in high yield (75-95% yield) and purity (>95%) through direct reaction of 3-(1H-tetrazol-5-yl) aniline and the appropriate sulfonyl chloride in dichloromethane at room temperature for 3 hours (Fig. 11).

1b Ar: 3-F-C_6H_4-
2b Ar: 3-NO_2-C_6H_4-
3b Ar: Dansyl-
4b Ar: 4-(CH_3CONH-)C_6H_4-
5b Ar: 8-Quinoline-
6b Ar: 4-Cl-C_6H_4-
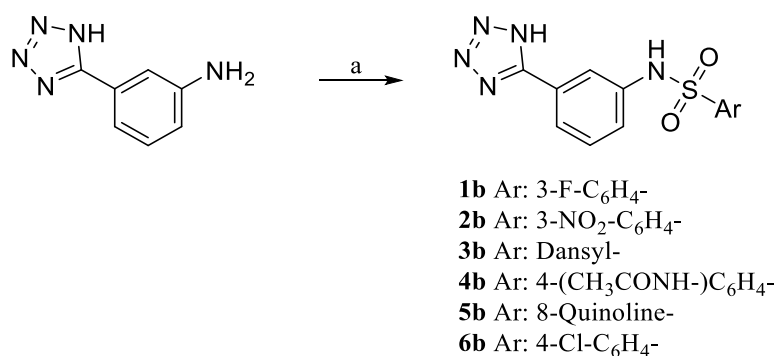
Figure 11. Reagents and conditions. a) aryl-sulfonyl chloride (1.2 eq.), pyridine (3 eq.), dry DCM, N_2, r.t, 3 h, 75-95% yield.

23

361   The derivatives of compound **11a** were tested for KPC-2 affinity (Table 3). They exhibited either weaker

362   activities than **11a** or were not active at all at tested concentration. Thus, it appeared that the sulfonamide

363   linker is not a suitable group to optimize the affinity of this compound series.

364

365   The antimicrobial activity of the best hits **9a** and **11a** and their derivatives was studied in bacterial cell

366   cultures to investigate their ability to cross the outer membrane reaching the periplasmic space, where

367   KPC-2 is secreted and confined in Gram negative bacteria. Compounds were tested for synergy with the

368   β-lactam antibiotic meropenem against four *K. pneumoniae* clinical strains, isolated from different

369   patients at the Hospital Universitario Son Espases, Palma de Mallorca, Spain. One of the four clinical

370   strains was not a KPC-2 producer and was susceptible to meropenem (strain **Kpn (C-)**; MIC <0.25

371   ug/mL). The three additional strains harbored the blaKPC-2 gene and were resistant to meropenem

372   (Table 4). [32] Noteworthy none of the tested compounds had intrinsic antibiotic activity (MIC >256

373   ug/mL), against the employed strains, included the susceptible one. The results show that in most cases

374   the compounds were not able to reverse antibiotic resistance and did not showed synergism with

375   meropenem. However, against strain Kpn 53A8 the MIC value was lowered by a factor of two when

376   meropenem was combined with compounds **32a**, **1b**, **2b**, **5b** and **6b** while in combination with

377   compound **11a** the MIC value was reduced by 4 fold.

378

379   **Table 4**: *In vitro* interaction between meropenem and synthesized compounds vs *K. pneumoniae*
380   clinical strains.

MIC[a] meropenem **in combination with synthesized compounds (1:1 molar)** [a, b, c] (µg/mL)				
Code	Kpn (C-)	Kpn 99D8	Kpn 53A8	Kpn 53A9
--	<0.25	256	256	256
9a	<0.25	256	256	256
11a	<0.25	256	64	256
32a	<0.25	256	128	256
1b	<0.25	256	128	256
2b	<0.25	256	128	256
4b	<0.25	256	256	256
5b	<0.25	256	128	256
6b	<0.25	256	128	256

381   [a] Assays were conducted against four *K. pneumoniae* clinical strains isolated from different patients at the
382   Hospital Universitario Son Espases, Palma de Mallorca, Spain. MICs were determined according to EUCAST
383   standards and the presented values are the median of three independent experiments.
384   [b] Compounds were testes alone and showed no activity (MIC>256) in all cases.
385   [c] Strain C- is control *K. pneumoniae* and meropenem susceptible (MIC < 0.25 ug/ml)

Conclusions

386

387 In this study two novel KPC-2 inhibitors were identified via an *in-silico* approach. 14 novel tetrazole

388 derivatives originating from the best, low micromolar, hit **11a** were designed, synthesized and evaluated

389 for their ability to inhibit KPC-2. We introduced chemical diversity on the distal part of the inhibitor,

390 choosing to keep unchanged the anchor tetrazole ring while modifying the amide and the distal ring.

391 The results suggests that a sulfonamide linker is not suitable to improve the potency of **11a**. Future

392 optimization work should instead rather concentrate on exploring secondary binding sites more distal

393 from the pocket that the screening hits are supposed to address [42]. If the amide functionally found in

394 **11a** or alternative linkers are best suited remains to be explored. Nevertheless, two promising hit

395 compounds for KPC-2 were retrieved which can serve as starting points to derive more potent inhibitors.

396 Although a decrease of potency in *in vitro* tests was registered for the designed and synthesized chemical

397 entities, as none of the compounds was able to trigger stronger interactions with the open region of KPC-

398 2 they were meant to target, this study yielded a better comprehension of the catalytic pocket of this

399 enzyme. Our study provided a better understanding of how challenging the target of additional,

400 superficial, binding pockets is and how it could be critical in designing inhibitors with improved

401 potency, especially in area proximal to the active site opening.

402 The (1H-tetrazol-5-yl)phenyl ring was most frequents among the high scoring candidates in our *in silico*

403 study, suggesting that this functionality is well suited to anchor ligands in the in KPC-2 binding site.

404 The rather weak affinity of the ligands hints that rest of the ligand, i.e. the functional groups out of the

405 center phenyl ring and the amide liker, need to be optimized to increase potency. However, introducing

406 a sulfonamide linker was detrimental for potency. We hypothesize that the presence of a sulfonamide

407 instead of an amide led to a rearrangement of the ligand in the binding site to minimize steric hindrance,

408 and thus resulted in the loss of key interactions. These rearrangements can be particularly critical in non-

409 covalent inhibitors like ours that are not stabilized by a covalent interaction with the catalytic serine, as

410 this type of inhibitors are supposed to have lower residence times with respect to covalent β-lactamase

411 inhibitors (Fig.1). In designing larger and more potent inhibitors, additional secondary binding sites

412 which have been found to be critical for affinity improvement need to be considered [42]. Further

413   medicinal chemistry work is ongoing to significantly increase the potency of the most promising

414   compound **11a** *in vitro* and *in vivo* and new chemistry is under evaluation for these derivatives, taking

415   advantage of other additional recognition sites in KPC-2.

416

Acknowledgements

Funding

References

427   1.   Papp-Wallace KM, Endimiani A, Taracila MA, Bonomo RA. Carbapenems: Past, present, and

428   future. Antimicrob Agents Chemother. 2011;55: 4943–4960. doi:10.1128/AAC.00296-11

429   2.   Tondi D, Cross S, Venturelli A, Costi MP, Cruciani G, Spyrakis F. Decoding the Structural

430   Basis For Carbapenem Hydrolysis By Class A beta-lactamases: Fishing For A Pharmacophore.

431   Curr Drug Targets. Netherlands; 2016;17: 983–1005.

432   3.   Livermore DM, Woodford N. The beta-lactamase threat in Enterobacteriaceae, Pseudomonas

433   and Acinetobacter. Trends Microbiol. England; 2006;14: 413–420.

434   doi:10.1016/j.tim.2006.07.008

435   4.   Farina D, Spyrakis F, Venturelli A, Cross S, Tondi D, Paola Costi M. The Inhibition of

436   Extended Spectrum β-Lactamases: Hits and Leads. Current Medicinal Chemistry. 2014; 21:

437   1405–1434

438   5.   Frère J-M, Sauvage E, Kerff F. From "An Enzyme Able to Destroy Penicillin" to

439   Carbapenemases: 70 Years of Beta-lactamase Misbehaviour. Current Drug Targets. 2016;17:

440   974–982

441 6.   Naas T, Dortet L, I. Iorga B. Structural and Functional Aspects of Class A Carbapenemases.

442   Current Drug Targets. 2016;17: 1006–1028.

443 7.   Papp-Wallace KM, Bethel CR, Distler AM, Kasuboski C, Taracila M, Bonomo RA. Inhibitor

444   resistance in the KPC-2 beta-lactamase, a preeminent property of this class A beta-lactamase.

445   Antimicrob Agents Chemother. United States; 2010;54: 890–897. doi:10.1128/AAC.00693-09

446 8.   Brem J, Cain R, Cahill S, McDonough MA, Clifton IJ, Jiménez-Castellanos J-C, et al.

447   Structural basis of metallo-β-lactamase, serine-β-lactamase and penicillin-binding protein

448   inhibition by cyclic boronates. Nat Commun. 2016;8: 12406.

449 9.   Santucci M, Spyrakis F, Cross S, Quotadamo A, Farina D, Tondi D, et al. Computational and

450   biological profile of boronic acids for the detection of bacterial serine- and metallo-β-

451   lactamases. Sci Rep. 2017;7: 1–15. doi:10.1038/s41598-017-17399-7

452 10.   Danishuddin M, Khan AU. Structure based virtual screening to discover putative drug

453   candidates: Necessary considerations and successful case studies. Methods. 2015;71: 135–145.

454   doi:https://doi.org/10.1016/j.ymeth.2014.10.019

455 11.   Khan A, Faheem M, Danishuddin M, Khan AU. Evaluation of Inhibitory Action of Novel Non

456   β-Lactam Inhibitor against Klebsiella pneumoniae Carbapenemase (KPC-2). PLoS One.

457   2014;9: e108246.

458 12.   Krishnan NP, Nguyen NQ, Papp-Wallace KM, Bonomo RA, van den Akker F. Inhibition of

459   Klebsiella β-Lactamases (SHV-1 and KPC-2) by Avibactam: A Structural Study. PLoS One.

460   2015;10: e0136813.

461 13.   Pemberton OA, Zhang X, Chen Y. Molecular Basis of Substrate Recognition and Product

462   Release by the Klebsiella pneumoniae Carbapenemase (KPC-2). J Med Chem. 2017;60: 3525–

463   3530. doi:10.1021/acs.jmedchem.7b00158

464 14.   Congreve M, Carr R, Murray C, Jhoti H. A "rule of three" for fragment-based lead discovery?

465   Drug Discov Today. 2003;8: 876–877.

466 15.   Ito JI, Tabei Y, Shimizu K, Tsuda K, Tomii K. PoSSuM: A database of similar protein-ligand

27

467   binding and putative pockets. Nucleic Acids Res. 2012;40: 541–548. doi:10.1093/nar/gkr1130

468   16.   Ito JI, Ikeda K, Yamada K, Mizuguchi K, Tomii K. PoSSuM v.2.0: Data update and a new

469   function for investigating ligand analogs and target proteins of small-molecule drugs. Nucleic

470   Acids Res. 2015;43: D392–D398. doi:10.1093/nar/gku1144

471   17.   Ke W, Bethel CR, Papp-Wallace KM, Pagadala SRR, Nottingham M, Fernandez D, et al.

472   Crystal structures of KPC-2 beta-lactamase in complex with 3-nitrophenyl boronic acid and

473   the penam sulfone PSR-3-226. Antimicrob Agents Chemother. 2012;56: 2713–2718.

474   doi:10.1128/AAC.06099-11

475   18.   Nichols DA, Jaishankar P, Larson W, Smith E, Liu G, Beyrouthy R, et al. Structure-based

476   design of potent and ligand-efficient inhibitors of CTX-M class A β-lactamase. J Med Chem.

477   2012;55: 2163–2172. doi:10.1021/jm2014138

478   19.   Tomanicek SJ, Standaert RF, Weiss KL, Ostermann A, Schrader TE, Ng JD, et al. Neutron and

479   X-ray Crystal Structures of a Perdeuterated Enzyme Inhibitor Complex Reveal the Catalytic

480   Proton Network of the Toho-1 β-Lactamase for the Acylation Reaction. J Biol Chem. 2013;15:

481   4715-4722

482   20.   Chen Y, Shoichet BK. Molecular docking and ligand specificity in fragment-based inhibitor

483   discovery. Nat Chem Biol. 2009;5: 358–364. doi:10.1038/nchembio.155

484   21.   Fonseca F, Chudyk EI, van der Kamp MW, Correia A, Mulholland AJ, Spencer J. The Basis

485   for Carbapenem Hydrolysis by Class A β-Lactamases: A Combined Investigation using

486   Crystallography and Simulations. J Am Chem Soc. American Chemical Society; 2012;134:

487   18275–18285. doi:10.1021/ja304460j

488   22.   Ambler RP, Coulson AF, Frere JM, Ghuysen JM, Joris B, Forsman M, et al. A standard

489   numbering scheme for the class A beta-lactamases. The Biochemical journal. England;

490   1991;15: 269–270.

491   23.   Brenk R, Schipani A, James D, Krasowski A, Gilbert IH, Frearson J, et al. Lessons learnt from

492   assembling screening libraries for drug discovery for neglected diseases. ChemMedChem.

493   2008;3: 435–444. doi:10.1002/cmdc.200700139

494   24.   Hawkins PCD, Skillman AG, Warren GL, Ellingson BA, Stahl MT. Conformer Generation

495   with OMEGA: Algorithm and Validation Using High Quality Structures from the Protein

496   Databank and Cambridge Structural Database. J Chem Inf Model. 2010;50: 572–584.

497   doi:10.1021/ci100031x

498 25.   Mpamhanga CP, Spinks D, Tulloch LB, Shanks EJ, Robinson DA, Collie IT, et al. One

499   scaffold, three binding modes: Novel and selective pteridine reductase 1 inhibitors derived

500   from fragment hits discovered by virtual screening. J Med Chem. 2009;52: 4454–4465.

501   doi:10.1021/jm900414x

502 26.   Brenk R, Irwin JJ, Shoichet BK. Here Be Dragons: Docking and Screening in an Uncharted

503   Region of Chemical Space. J Biomol Screen. 2005;10: 667–674.

504   doi:10.1177/1087057105281047

505 27.   Mysinger MM, Shoichet BK. Rapid context-dependent ligand desolvation in molecular

506   docking. J Chem Inf Model. 2010;50: 1561–1573. doi:10.1021/ci100214a

507 28.   Lorber DM, Shoichet BK. Flexible ligand docking using conformational ensembles. Protein

508   Sci. 1998;7: 938–950.

509 29.   Wei BQ, Baase WA, Weaver LH, Matthews BW, Shoichet BK. A Model Binding Site for

510   Testing Scoring Functions in Molecular Docking. J Mol Biol. 2002;322: 339–355.

511   doi:10.1016/S0022-2836(02)00777-5

512 30.   Kuntz ID, Chen K, Sharp KA, Kollman PA. The maximal affinity of ligands. Proc Natl Acad

513   Sci. 1999;96: 9997–10002.

514 31.   Hopkins AL, Groom CR, Alex A. Ligand efficiency : a useful metric for lead selection. Drug

515   Discov Today. 2004;9: 430–431.

516 32.   Celenza G, Vicario M, Bellio P, Linciano P, Perilli M, Oliver A, et al. Phenylboronic Acid

517   Derivatives as Validated Leads Active in Clinical Strains Overexpressing KPC-2: A Step

518   against Bacterial Resistance. ChemMedChem. 2018; doi:10.1002/cmdc.201700788

519 33.   Crompton R, Williams H, Ansell D, Campbell L, Holden K, Cruickshank S, et al. Oestrogen

520   promotes healing in a bacterial LPS model of delayed cutaneous wound repair. Lab Invest.

521   United States; 2016;96: 439–449. doi:10.1038/labinvest.2015.160

522 34.   Feng BY, Shoichet BK. A detergent-based assay for the detection of promiscuous inhibitors.

523   Nat Protoc. 2006;1: 550–553. doi:10.1038/nprot.2006.77

524   35.   Quotadamo A, Linciano P, Davoli P, Tondi D, Costi MP, Venturelli A. An Improved Synthesis

525   of CENTA, a Chromogenic Substrate for β-Lactamases. Synlett. 2016;27: 2447–2450.

526   doi:10.1055/s-0035-1562454

527   36.   Cheng Y, Prusoff WH. Relationship between the inhibition constant (K1) and the concentration

528   of inhibitor which causes 50 per cent inhibition (I50) of an enzymatic reaction. Biochem

529   Pharmacol. England; 1973;22: 3099–3108.

530   37.   Strynadka NC, Adachi H, Jensen SE, Johns K, Sielecki A, Betzel C, et al. Molecular structure

531   of the acyl-enzyme intermediate in beta-lactam hydrolysis at 1.7 A resolution. Nature.

532   1992;359: 700–705. doi:10.1038/359700a0

533   38.   Tondi D, Venturelli A, Bonnet R, Pozzi C, Shoichet BK, Costi MP. Targeting class A and C

534   serine beta-lactamases with a broad-spectrum boronic acid derivative. J Med Chem.2014;57:

535   5449–5458. doi:10.1021/jm5006572

536   39.   Genovese F, Lazzari S, Venturi E, et al (2017) Design, synthesis and biological evaluation of

537   non-covalent AmpC β-lactamases inhibitors. Med Chem Res 26:975–986 . doi:

538   10.1007/s00044-017-1809-x

539   40.   Seidler J, McGovern SL, Doman TN, Shoichet BK. Identification and Prediction of

540   Promiscuous Aggregating Inhibitors among Known Drugs. J Med Chem. 2003;46: 4477–4486.

541   doi:10.1021/jm030191r

542   41.   Vijayadas KN, Davis HC, Kotmale AS, Gawade RL, Puranik VG, Rajamohanan PR, et al. An

543   unusual conformational similarity of two peptide folds featuring sulfonamide and carboxamide

544   on the backbone. Chem Commun. The Royal Society of Chemistry; 2012;48: 9747–9749.

545   doi:10.1039/C2CC34533A

546   42.   Babaoglu K, Shoichet BK. Deconstructing fragment-based inhibitor discovery. Nature

547   chemical biology.2006;2: 720–723. doi:10.1038/nchembio831

548